


Research Article

Early Identifying and Monitoring Landslides in Guizhou Province with InSAR and Optical Remote Sensing

Genger Li,^{1,2} Bo Hu ,^{1,3} Hui Li,⁴ and Feng Lu ¹

¹Surveying Engineering, Guangdong University of Technology, Guangzhou 510006, China

²Guangdong Institute of Geological Surveying and Mapping, Guangzhou 510815, China

³Innovation Academy for Precision Measurement Science and Technology, Chinese Academy of Sciences, Wuhan 430077, China

⁴Guangdong Hydropower Planning & Design Institute (GPDI), 116 Tianshou Road, Tianhe District, Guangzhou, China

Correspondence should be addressed to Bo Hu; hubo@asch.whigg.ac.cn

Received 4 December 2020; Revised 22 April 2021; Accepted 5 May 2021; Published 1 July 2021

Academic Editor: Giuseppe Maruccio

Copyright © 2021 Genger Li et al. This is an open access article distributed under the Creative Commons Attribution License, which permits unrestricted use, distribution, and reproduction in any medium, provided the original work is properly cited.

The topography and landforms of Guizhou Province in China are complicated, and the climatic conditions of heavy precipitation make landslide disasters in Guizhou Province occur frequently. To avoid damage to people's lives and economic property caused by disasters, a reliable early landslide identification method and landslide monitoring method are urgently needed. Traditional landslide identification and monitoring methods have limitations. InSAR technology has unique advantages in large-scale landslide identification and monitoring, but landslide identification results based on a single deformation value are one-sided. Therefore, this paper uses Sentinel-1A radar satellite image data and uses InSAR technology and optical remote sensing technology to carry out large-scale surface deformation monitoring and identification of dangerous deformation areas in Liupanshui City, Tongren City, Guiyang City and other regions in Guizhou Province. The potential landslide identification methods based on the time series normalized difference vegetation index and landslide development environment elements are combined to investigate hidden landslide hazards in the study area. In this paper, time series InSAR technology is used to monitor three key landslides in Jichang Town, Yujiaying and Fana, to grasp the movement status of the landslide in time. The method of landslide identification and monitoring in this paper is of great significance for disaster prevention and management in Guizhou Province.

1. Introduction

China is a country where geological disasters occur frequently. In addition to earthquakes, landslides are one of the most natural disasters that threaten the lives and property of the country and people. Especially in Guizhou Province, landslides are the main geological disasters in Guizhou Province because of its complex topography, location at the junction of tectonic plates, frequent human infrastructure activities, and climate conditions. In recent years, the number of deaths and disappearances caused by landslide disasters in Guizhou Province has been at the forefront of the country, and the economic losses caused by disasters have been huge. Therefore, in order to mitigate the losses caused by landslides, early identification and monitoring of landslides are urgently needed. At present, the commonly used landslide

identification and monitoring methods are generally traditional measurement methods or field surveys. The monitoring results obtained by these methods are all based on single-point measurement results, and require a lot of manpower and financial resources. These methods are high-risk and low-efficiency, and lack of continuous macro-monitoring of disaster-prone areas. Optical remote sensing technology has the advantages of large coverage and recognition by human-computer interaction in identifying and monitoring landslides, and the accuracy of the recognition results is high [1]. Many scholars have done a lot of work in landslide identification by using optical remote sensing technology [2–4]. However, when remote sensing technology is used to identify landslides in a large area, the interpretation takes a long time and a large workload. InSAR technology is very sensitive to small deformation information, it has the

advantages of non-contact measurement, not affected by weather conditions, high-precision monitoring and so on. With the continuous launch of radar satellites and the increasing perfection of InSAR processing technology, the accuracy of surface deformation results obtained using InSAR technology has also increased. Reliable monitoring results make InSAR technology more and more used in the field of landslide research [5, 6]. Especially time series InSAR technology can reverse the deformation process of landslide with time [7–12]. But InSAR technology is susceptible to deformation gradient and vegetation growth. In addition, due to different causes of deformation signals, the results of using surface deformation values to identify landslides are one-sided, which poses technical difficulties for conventional InSAR technology to identify and monitor landslides. Therefore, there is an urgent need to explore methods for early identification and monitoring of landslides in a large area. Judging from the current research progress, a single discipline or method can no longer meet the needs of landslide research. The integration of multiple disciplines and methods is the trend of landslide identification and prevention research. In this paper, InSAR technology and optical remote sensing technology are combined to identify and classify dangerous deformation zones. Then this paper comprehensively uses the landslide development environment elements analysis technology and the normalized difference vegetation index (NDVI) time series analysis technology to identify potential landslides. This paper also uses the InSAR method to monitor the deformation of key landslides. By extracting the deformation information of the landslide to analyze the stable state, formation mechanism and possible causes of the landslide. This article is of great significance for landslide disaster monitoring and early warning, regional disaster prevention and mitigation, and can provide technical reference for landslide disaster research in similar regions.

2. Study Area and Data

2.1. Overview of Study Area. Guizhou Province is located on the Yunnan-Guizhou Plateau in southwestern China, with latitudes ranging from $24^{\circ}37'N$ to $29^{\circ}13'N$ and longitudes ranging from $103^{\circ}36'E$ to $109^{\circ}35'E$, with an area of approximately 176,200 km². The average altitude is around 1100 m. Guizhou has a subtropical monsoon climate. There is sufficient precipitation in Guizhou Province, and precipitation is mainly concentrated in summer. The landform types in Guizhou are mainly plateau and mountainous areas, and there are also typical karst landforms. Due to the influence of tectonic movements in Guizhou, the landform types vary greatly, which makes the distribution quantity, severity and scale of landslides in Guizhou Province have obvious differences. This paper mainly selects Liupanshui City, Guiyang City, and Tongren City among the landslide-prone cities in Guizhou Province as the research area.

2.2. Data. The radar satellite image data used in this article is Sentinel-1A satellite data. The radar imaging satellite is the first dual-constellation satellite developed by ESA and the European Commission for the Copernicus Earth Observa-

tion Project. The revisit period for the Sentinel series satellite single constellation is 12 days, and the revisit period for the dual constellation cooperative work is 6 days. Sentinel-1A satellite imaging modes include Stripmap Mode (SM), Interferometric Wide Swath mode (IW), Wave mode (WV) and Extra Wide Swath Mode (EW) [13]. This article uses Sentinel-1A radar satellite data in IW mode. The data width is 250 km, and the incident angle is 29° to 46° . The resolution of the data is 5×20 m. The detailed information of Sentinel-1A radar satellite image data used in this paper is shown in Table 1. The data coverage is shown in Figures 1–3, respectively.

In this paper, the ALOS World 3D-30 m Digital Elevation Model (AW3D30 DEM) data is used as the basic ground elevation information data for this study. In May 2015, the Japan Aerospace Exploration Agency (JAXA) released AW3D30 DEM data, which was obtained through the PRISM panchromatic stereo mapping sensor PRISM on ALOS. The coverage of this data ranges from $82^{\circ}N$ to $82^{\circ}N$. AW3D30 DEM data is 30 m resolution DEM data obtained by resampling 5 m resolution DEM data. AW3D30 DEM data is currently more accurate DEM data.

This article selects MODIS 13Q1 data for extracting NDVI value. The spatial resolution of MOD13Q1 data is 250 m, the data adopts the maximum value synthesis method, and the data period is 16 days. In this paper, the row number of the data area is h27v06, the data set version number is V005, and the data acquisition time is from January 01, 2017 to September 14, 2019, a total of 63 images. The data can be downloaded from the NASA website. It is MOD13Q1 data in HDF format that contains information such as data structure and data location. MODIS13Q1 products contain 12 bands, including NDVI values, which can be used for global vegetation status monitoring and land cover changes.

In the process of InSAR data processing, due to the existence of orbit errors that will affect the interference results, the precise orbit information is required in the steps of image registration and data import. The orbit data selected in this paper is POD precise orbital ephemeris data, and its positioning accuracy is higher than 5 cm, which is currently the most accurate satellite orbit data.

3. Method and Data Processing

In 2002, Berlendino et al. proposed a new time series InSAR analysis method [14], the Small Baseline Subsets (SBAS) method. SBAS technology uses the principle of small baseline length in the data set to constrain the time baseline and space baseline of all interference image pairs, and freely combines the SAR data obtained by remote sensing satellites into a small baseline data set. Then, the Least Square method (LS) is used to obtain a time series of surface deformation in each small baseline data set. Then use the SVD method to combine a series of small baseline sets to find the minimum norm solution of the deformation rate, solve the problem of rank deficit of the total equation, and obtain long-term sequence deformation. In the SBAS method, the phase unwrapping is generally performed by the Minimum Cost Flow algorithm.

TABLE 1: SENTINEL-1A Data Used in This Study.

Study area	Number	Ascending/descending	Data
Guiyang	60	Ascending	20170327-20190621
Liupanshui	32	Ascending	20180806-20190813
	32	Descending	20180808-20190827

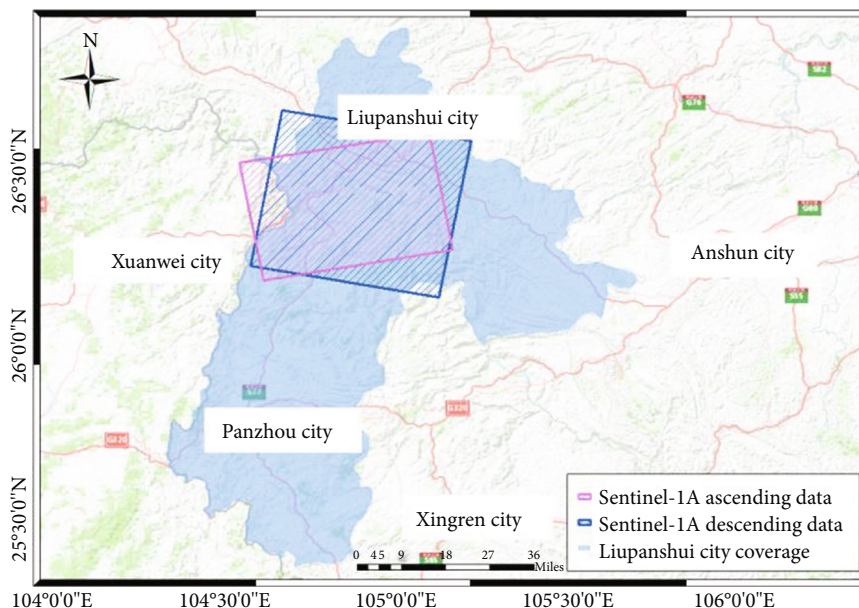


FIGURE 1: Coverage map of Sentinel-1A data in Liupanshui city.

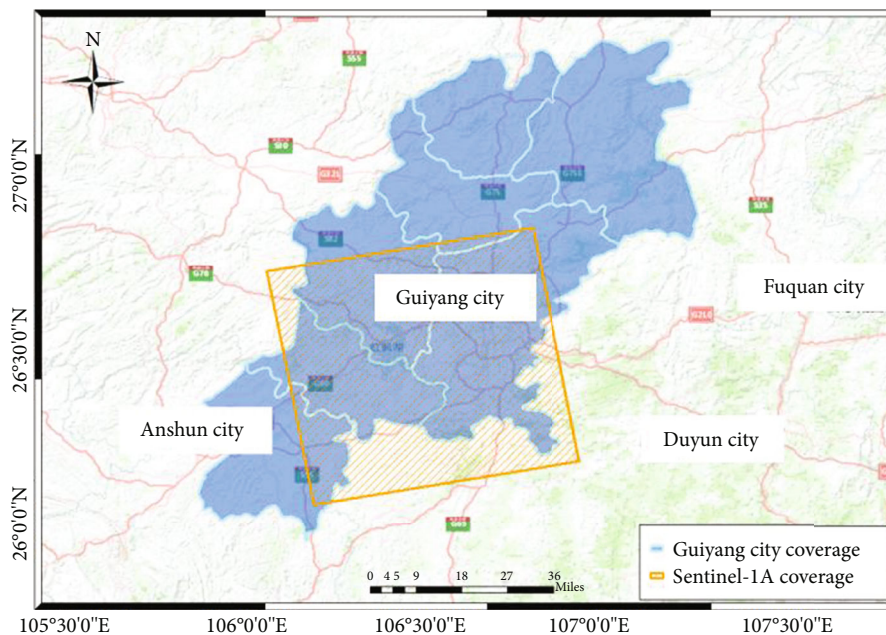


FIGURE 2: Coverage map of Sentinel-1A data in Guiyang city.

SBAS technology can overcome the spatial de-correlation problem caused by the long baseline. It can also improve the time sampling rate of the data and has a higher spatial

measurement density. There are mainly the following steps to obtain surface deformation through SBAS InSAR technology processing:

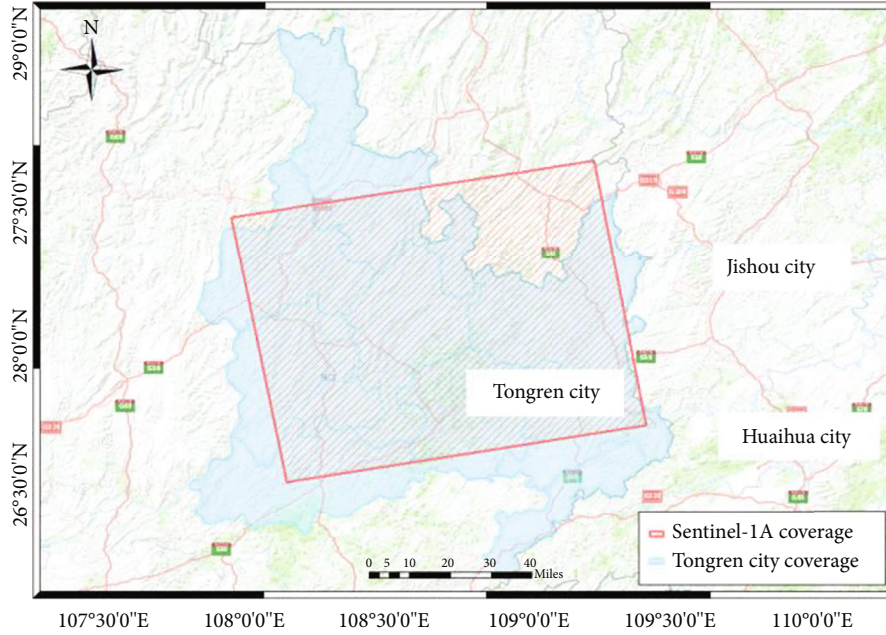


FIGURE 3: Coverage map of Sentinel-1A data in Tongren city.

TABLE 2: Baseline Threshold Parameters.

Study area	Time baseline threshold (day)	Spatial baseline threshold (%)	Interference pair
Liupanshui (ascending)	100	45	220
Liupanshui (descending)	150	30	169
Guiyang	100	20	258
Tongren	90	30	156

3.1. Generate Connection Diagram. In this step, all the acquired SAR data needs to be input, and all SAR data are paired through the optimal combination method. Generally, different time baseline and space baseline thresholds are set according to the characteristics of the study area to generate interference image pairs. The baseline threshold parameters and image pair connections set for the study area in this article are shown in Table 2.

3.2. Interference Processing. Before generating an interferogram, first register the acquired image, and then generate the interferogram. The interferogram should be processed to eliminate the terrain phase processing and phase unwrapping to obtain the initial interference image pair. In this paper, the unwrapping threshold is set to 0.28 during the interference process to improve unwrapping accuracy. The unwrapping method used is the Delaunay MCF method. This unwrapping method is suitable for a large number of areas with low coherence. The filtering method uses the Goldstein filter algorithm with a good filtering effect. In order to prevent oversampling and loss of deformation details, the unwrapping level is first taken to be a small value. In this paper, the unwrapping level is set to 1.

Before the refinement and re-flattening, the connectivity of the image pair is needed to be edited. The interference

image pairs with undesirable unwrapping effect, large orbit error, low coherence, and large atmospheric influence are eliminated. So that they will not participate in the subsequent processing work [15].

3.3. Refinement and Re-Flattening. This step requires the estimation and removal of some constant phase and phase jumps that still exist. The most important thing in this step is to select GCP points. The requirements for the selection of GCP are as stable as possible, without phase jumps and with good coherence. The optimized result of this step will be used as the input data of the first step of SBAS inversion.

3.4. SBAS Inversion. The first step of SBAS inversion is mainly to estimate the deformation rate, the residual terrain phase, and perform the unwrapping optimization of the interferogram to basically determine the position and range of the deformation. In this paper, the matching model type is Linear, because the model is the most robust. In the first step of the inversion process, it is also necessary to filter the coherent target by setting the coherence threshold. Only pixels larger than this threshold can participate in the calculation. In this paper, the unwrapping threshold and the coherence threshold are both set to 0.28. In order to remove the larger erroneous phase, the unwrapping level is increased to 2 in the first step inversion. The second step of SBAS

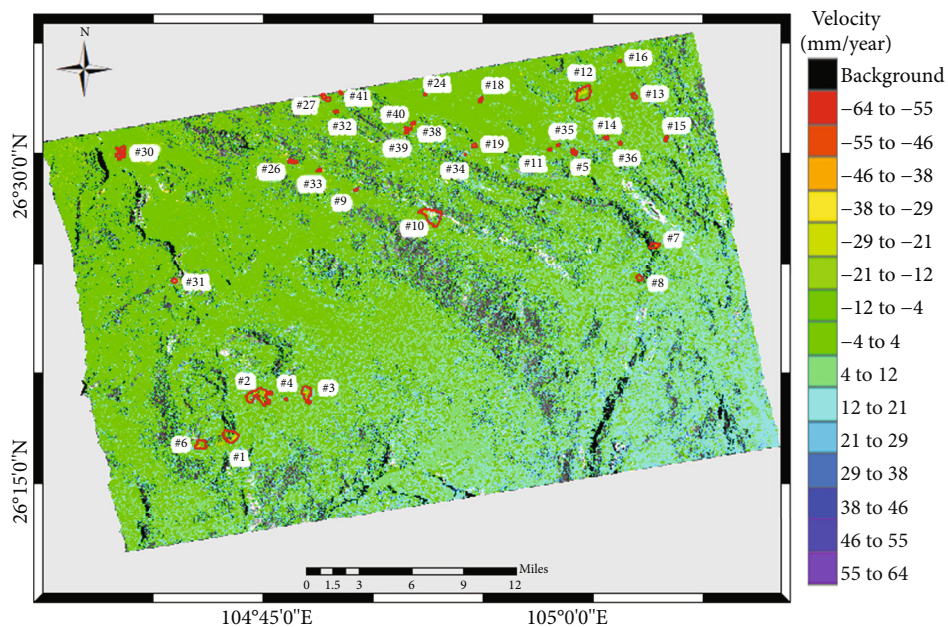


FIGURE 4: The average displacement rate map of ascending data in Liupanshui City (The red area is the dangerous deformation area).

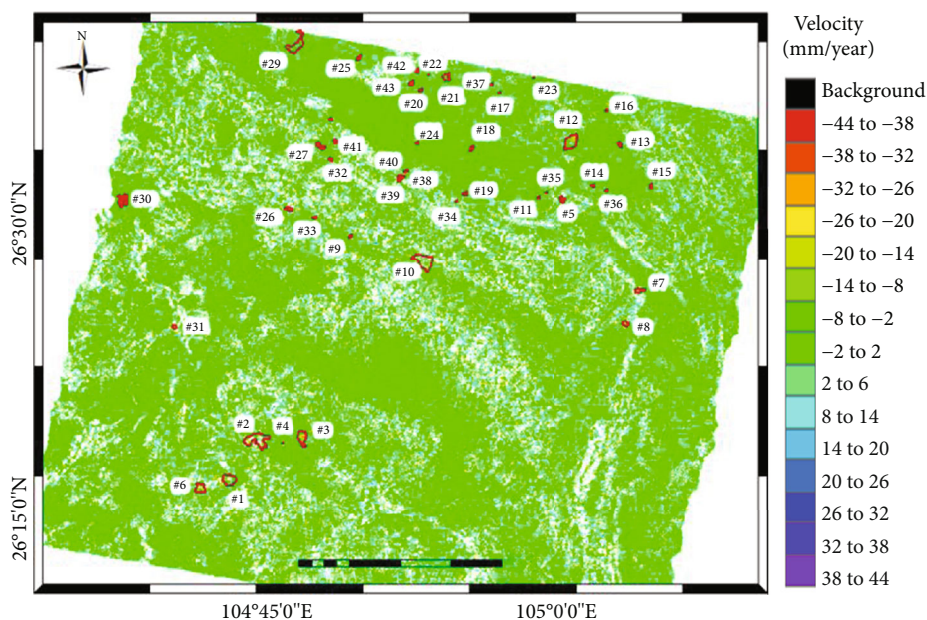


FIGURE 5: The average displacement rate map of descending data in Liupanshui City (The red area is the dangerous deformation area).

inversion is to remove the atmospheric phase to obtain the optimized rate value and obtain the time series deformation value. The removal of the atmospheric phase is achieved by low-pass and high-pass filtering.

3.5. *Geocoding.* This step is mainly to geocode the calculated results and reproject the deformation results and deformation rate into the LOS direction. The geocoding results can be analyzed for historical cumulative deformation, which is calculated based on the first phase.

4. Landslide Identification Results

4.1. *Extraction of Surface Deformation Areas Based on InSAR.* This paper uses SBAS technology to obtain the surface deformation information of Liupanshui City, Tongren City, Guiyang City and Guian New District. Figures 4–7 are the average displacement rate maps in the study area. It can be seen that the annual average displacement rate of the Liupanshui research area is between -64 mm/year and 64 mm/year, the annual average displacement rate of the Guiyang research

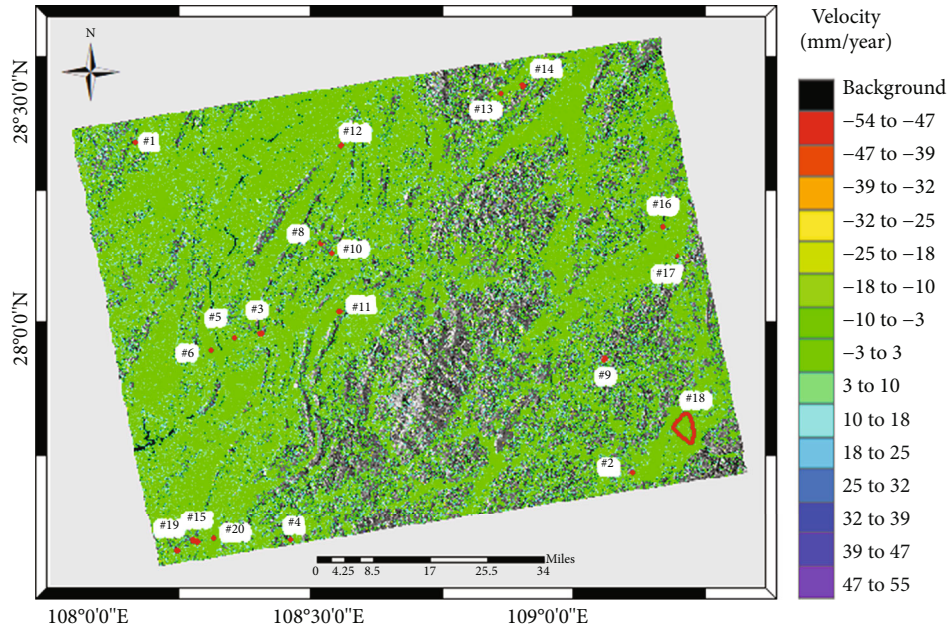


FIGURE 6: The average displacement rate map of Tongren City (The red area is the dangerous deformation area).

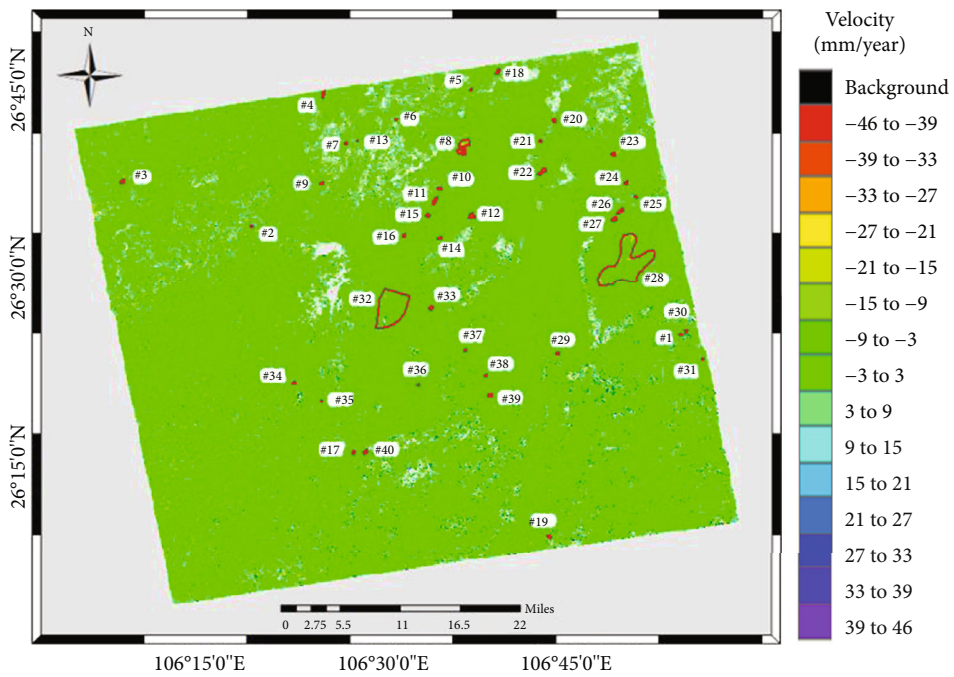


FIGURE 7: The average displacement rate map of Guiyang City (The red area is the dangerous deformation area).

area is between -46 mm/year and 37 mm/year, and the annual average displacement rate of the Tongren research area is between -54 mm/year and 47 mm/year. Based on the deformation rate information, this paper conducts a large-scale investigation of surface deformation in the study area. The area where the deformation level is large and the deformation rate exceeds -20 mm/year during the monitoring period, that is, the area where there is an obvious deformation signal is determined as a “dangerous deformation area”.

In this paper, 43 dangerous deformation areas were identified in the Liupanshui, 40 dangerous deformation areas were identified in the Guiyang, and 19 dangerous deformation areas were identified in the Tongren.

4.2. *Landslide Recognition Based on Optical Image.* Landslide is a natural phenomenon in which rocks and soil on a slope slide downward along the weak surface under the influence of gravity due to factors such as rainfall, groundwater, river

TABLE 3: Optical Remote Sensing Interpretation and Identification Signs of Landslides.

Identification signs	Image characteristics	
Direct identification signs	Geometry	Gentler than surrounding slope The slope is tongue-shaped or curved The back wall of the landslide Looks like a chair
	Color tone	Off-white Khaki Dark brown
	Texture	Rough Grainy Uneven
Indirect identification signs	Geomorphology	Fracture distribution Multi-layer terraces Mostly distributed in gully areas
	Slope vegetation	Low vegetation coverage And exposed rock mass
	Rivers, roads or buildings	Unnatural river turns or diversions

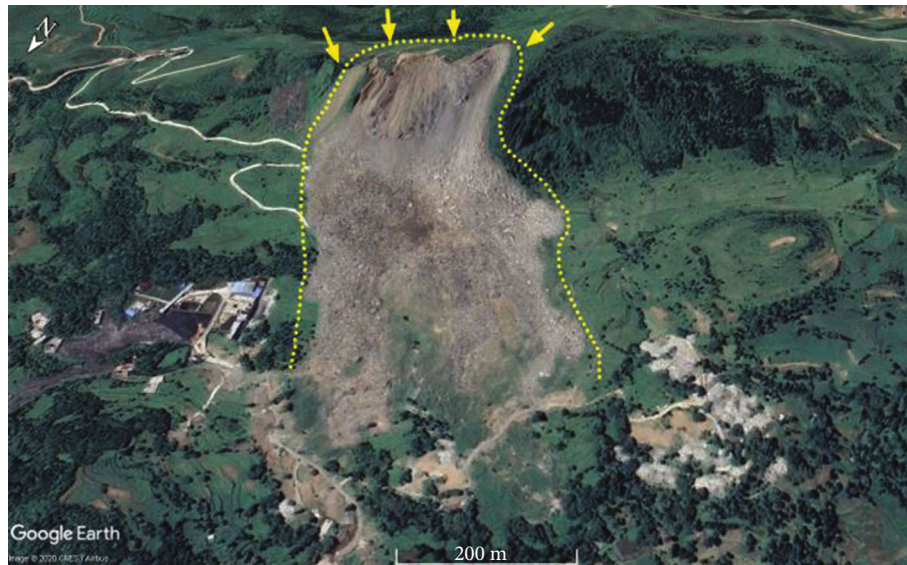
erosion, earthquakes, and human activities. As the landslide penetrates or obvious slip occurs, obvious landslide signs will appear, and these measurable signs are also called landslide elements. Landslide identification usually uses landslide elements for identification. Because when using optical remote sensing to interpret the landslide, only the surface information can be seen, and the underground part of the landslide cannot be seen. Therefore, in the remote sensing image recognition, it is necessary to have two elements of landslide wall and landslide body to be recognized as a landslide. This paper uses Google Earth optical images for landslide identification, which not only avoids the problem of cloud coverage in the study area, but also understands the process of landslide changes over time through historical archived images, which can provide a large amount of reliable data for landslide identification.

When using optical images to identify landslides, they are generally identified by direct identification signs and indirect identification signs. The direct identification signs include the hue, texture, and geometry of the landslide body. Indirect identification signs include changes in landform, slope vegetation, water system, landscape, etc. caused by landslides. Due to the different geological conditions and topography of the landslide, there are differences in the establishment of landslide identification signs. Therefore, this paper combines the characteristics of optical remote sensing images of typical landslides in Guizhou Province, and establishes optical remote sensing identification signs suitable for the study area, as shown in Table 3. The optical remote sensing images of typical landslides are shown in Figure 8.

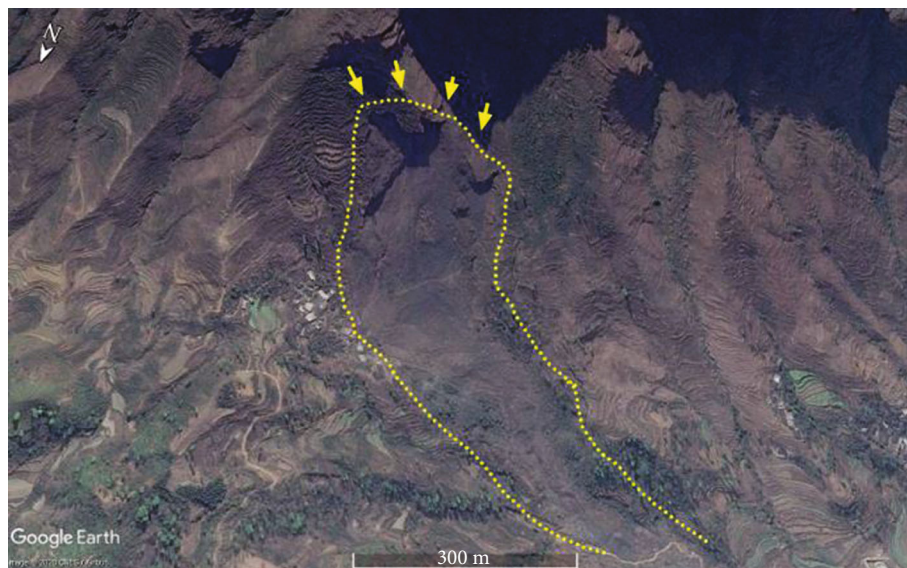
Based on Google Earth optical remote sensing image data, this paper uses landslide optical remote sensing interpretation signs to identify landslides in dangerous deformation zones extracted by SBAS technology. If the dangerous deformation area shows the image characteristics of landslide recognition on the optical image, the area is a landslide zone. If the dangerous deformation area can be clearly identified on the image as areas with frequent human activities such as dig-

ging and filling areas, construction areas or mining areas, these areas are judged as deformation areas caused by other reasons, and are called other deformation areas. If none of the above feature information is available, the area is determined to be a possible landslide area, and further landslide identification is needed. Figure 9 shows the results of landslide identification and classification in the Liupanshui study area. A total of 11 landslide areas, 3 areas where landslides may exist, and 29 other deformation areas are identified and determined. Figure 10 shows the identification results of the Guiyang study area. A total of 3 landslide areas, 1 area where landslides may exist, and 36 other deformation areas are identified and classified. Figure 11 shows the identification results of the research area in Tongren City. A total of 2 landslide areas, 10 areas where landslides may exist, and 7 other deformation areas were identified and determined.

4.3. Identification of Potential Landslides Based on NDVI Time Series Features. There is a difference in the ability of plants to reflect light. Combine the plant spectral data linearly and nonlinearly, and the resulting spectral index is the vegetation index. Nowadays, among the dozens of existing plant cover indexes, the vegetation index used commonly is the NDVI, which has a very strong ability to reflect vegetation information. The value range of NDVI is between -1 and 1. When the NDVI value is negative, the main coverings on the surface are clouds, snow, and water. When the NDVI value is close to 0, it means that the surface cover is mainly rock and bare soil. The NDVI value of the vegetation coverage area is positive. When the NDVI vegetation index value is larger, it means that the vegetation coverage of the area is higher. The method of using time series NDVI to identify potential landslides is mainly based on the close relationship between the landslide and the growth status of the slope vegetation. Generally speaking, areas with low vegetation coverage will weaken the stability of slopes and increase the probability of landslides. Therefore, areas with landslides usually have low NDVI values. Once a landslide occurs on



(a) Landslide in Zhangjiawan Town, Nayong County, Bijie City



(b) Landslide in Gangwu Town, Guanling County, Anshun City

FIGURE 8: Continued.



(c) Landslide in Qingtang Village, Daping Township, Wanshan District, Tongren City



(d) Landslide in Longchang Town, Kaili City

FIGURE 8: Google Earth remote sensing images of known landslides in Guizhou Province.

the slope body, the vegetation of the slope body in the affected area will be destroyed in a short time. The slope surface is mostly bare rock and accumulated clastic rock. The most obvious manifestation of this change of slope body is that the NDVI value of the slope body area is low, and the NDVI value decreases or even approaches 0 in a short time before the landslide occurs. Over time, the slope body and surrounding vegetation gradually recovered. This feature appears in the time series NDVI curve as NDVI slowly rises back to normal values in the late stage of the landslide. This is different from the seasonal growth characteristics of plants and mutations caused by the influence of clouds and aerosols.

In this paper, the NDVI value of the slope body in the possible landslide area is extracted, and the time series characteristics are analyzed to identify the slope body with a potential landslide. This paper is based on the relationship

between NDVI changes of landslide and slope vegetation time series. In the period of InSAR monitoring but not covered by the optical image, if the NDVI value of the slope vegetation is low or the NDVI time series curve drops sharply in the early stage and slowly rises in the later stage, the slope is identified as a potential landslide. Otherwise, it is judged as an unstable slope. In this paper, all the recognition and determination results of 14 slopes in the study area are shown in Table 4.

Through analysis and judgment, a total of 9 potential landslides are identified, and 1 is not a potential landslide. The 4 slopes cannot be accurately judged because of the deformation area of the slope. In order to increase the accuracy of landslide identification, it can be combined with other landslide identification methods for comprehensive identification.

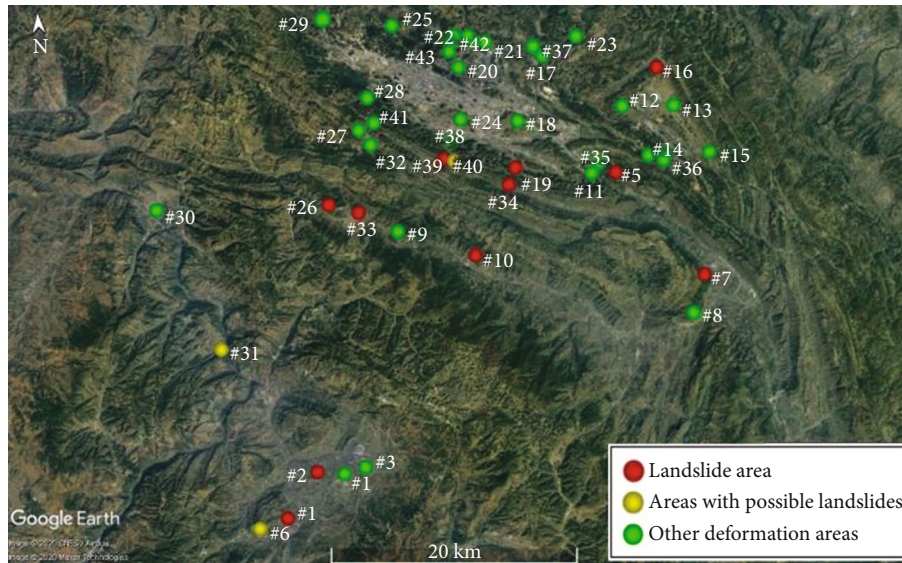


FIGURE 9: Distribution map of recognition results in Liupanshui Research Area.

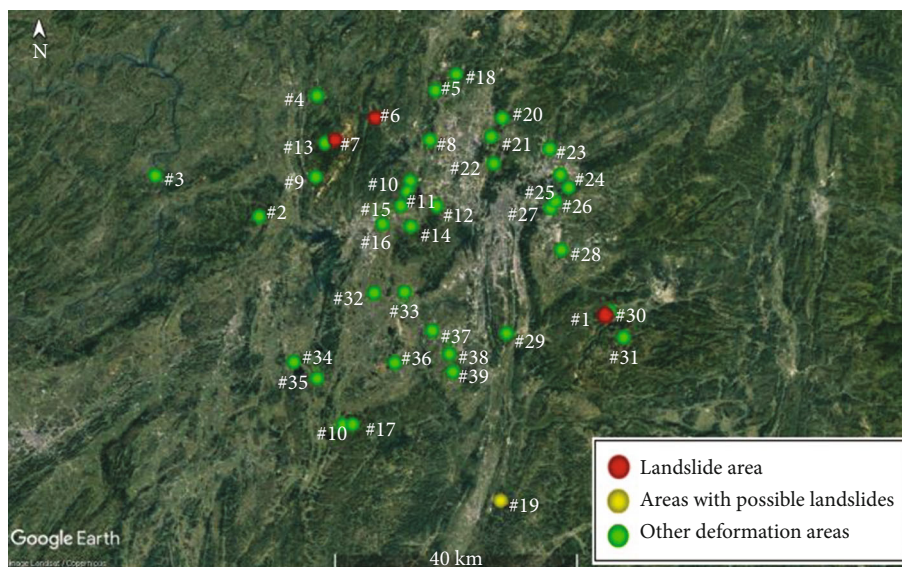


FIGURE 10: Distribution map of recognition results in Guiyang Research Area.

4.4. Identification of Potential Landslides Based on Environmental Factors of Landslide Development. In addition to external factors, the occurrence of landslides also needs some geographical conditions as the basic environmental elements for landslide development, including geological structure conditions, rock and soil conditions, groundwater conditions, topography and landform conditions, slope body cover conditions. Because the topography is the basic condition for the formation of landslides. Based on the existing research, this study selected four elements as slope, aspect, relief degree of land surface (RDLS) and surface roughness as the environmental factors for landslide development. In order to study the relationship between landslides and four elements in the three research areas of Guiyang City, Liupanshui City and Tongren City and their surrounding areas. This

paper uses DEM data to extract and grade the terrain slope, aspect, RDLS and roughness values.

The influence of topography and landform conditions on landslides in different regions is different. In order to comprehensively consider the contribution of special topography and landform conditions in Guizhou to landslides, this paper will base on the landslides identified by SBAS technology and optical remote sensing images. The characteristics of the environmental factors of landslide development in the study area are analyzed to ensure the accuracy of potential landslide identification. Aiming at the 16 landslides identified by optical remote sensing technology, this paper extracts four kinds of landslide development environment elements: aspect, slope, roughness and RDLS. Then count the number of landslides for each

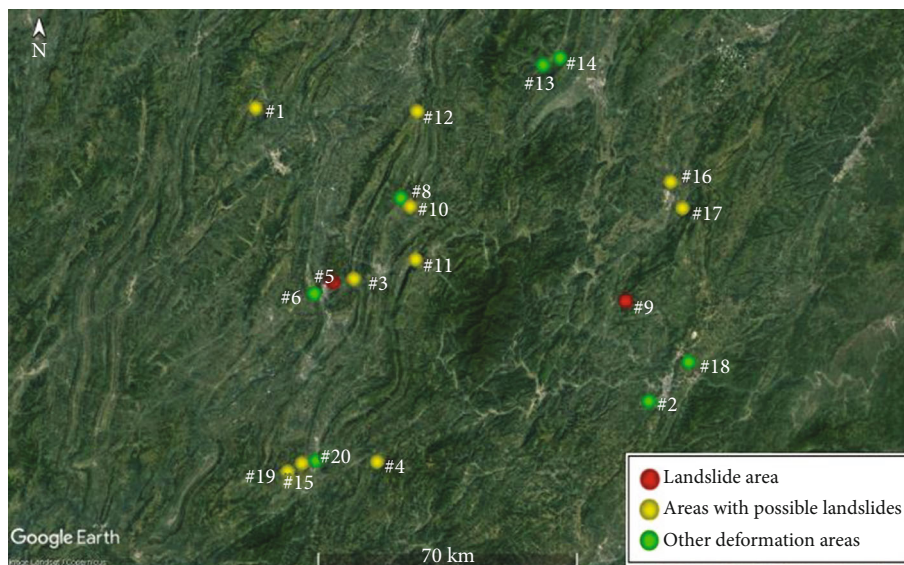


FIGURE 11: Distribution map of recognition results in Tongren Research Area.

TABLE 4: Identification Result of Possible Landslide Area Based on Time Series NDVI.

Landslide number	Study area	Variation characteristics of time series NDVI	Potential landslide (yes/no)
#6	Liupanshui	NDVI gradually decreased during the monitoring period	Yes
#31		Continuous decline in the short term, and then rebound to normal value in the later period	Yes
#39		During the monitoring period, the NDVI value continued to decrease	Yes
#19		During the monitoring period, the NDVI value decreased significantly in the short term, and then gradually returned to the normal value level	Yes
#1	Guian	There is no abnormal change in the NDVI value	No
#3		NDVI value is at a lower level compared to the same period in previous years	Yes
#4		During the monitoring period, the NDVI value has a tendency to decrease slowly, and a sudden drop in the later period occurs	Yes
#10			
#11	Tongren		
#12		Although the NDVI value is disturbed, the overall trend is decreasing continuously	Yes
#15		During the monitoring period, the NDVI curve showed a slow downward trend, and NDVI continued to be below 0.1 for a period of time	Yes
#16			
#17			
#19		During the monitoring period, NDVI fell suddenly, and remained at a level close to 0 in the later period.	Yes

element index after classification to obtain the reliable threshold range of development environment elements for landslides in Guizhou. The statistical results are shown in Figure 12.

Based on the landslides identified by optical remote sensing in the study area, according to the analysis of its developmental environmental factors, the topography slope of the slope body was selected between 20° and 60°, terrain relief > 120 m, terrain roughness > 1.1 as potential landslides

Filter threshold. Since the slope direction is distributed in all directions, the south and southeast directions are relatively more distributed, but the difference is not large. Therefore, the slope direction is only used as a reference index for the existence of potential landslides. In this paper, the above indexes are extracted from 14 areas where landslides may exist in the study area. If the index value of the slope body is within the screening threshold range, the potential landslide of this slope body is considered. Considering the

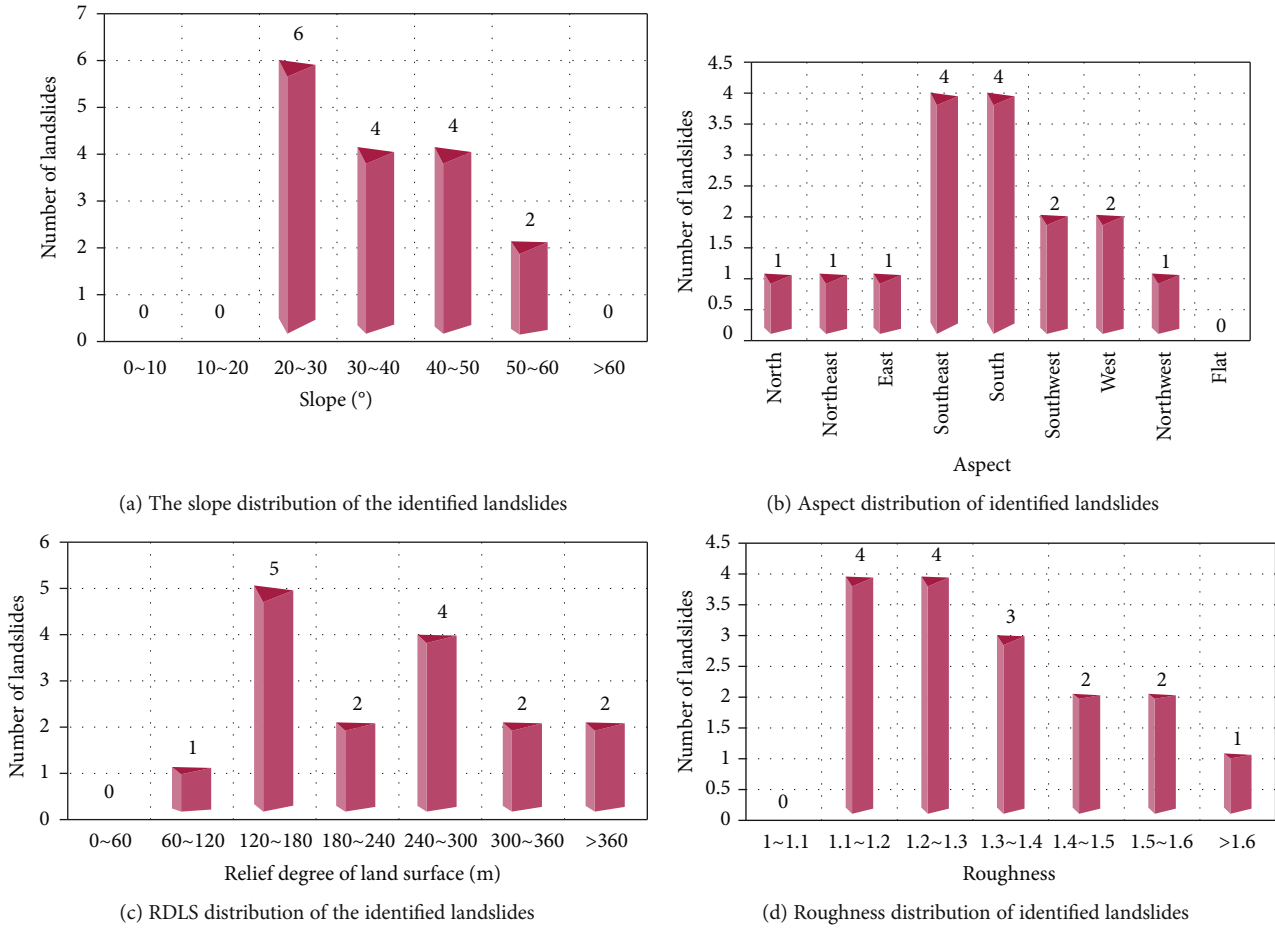


FIGURE 12: The statistic distribution map of landslide elements.

TABLE 5: Identification Results Based on Landslide Development Environment Elements.

Number	Landslide code	Slope (°)	Aspect	RDLS (m)	Roughness	Potential landslide (yes/no)	Study area
1	#6	>60	South	>360	>1.6	Yes	Liupan shui
2	#31	30-40	South	300-360	1.1-1.2	Yes	
3	#39	30-40	Southeast	180-240	1.2-1.3	Yes	
4	#19	20-30	East	180-240	1.2-1.3	Yes	Guiyang
5	#1	10-20	Southeast	60-120	1-1.1	No	Tongren
6	#3	20-30	East	120-180	1-1.1	Yes	
7	#4	30-40	South	180-240	1.1-1.2	Yes	
8	#10	10-20	East	60-120	1-1.1	No	
9	#11	40-50	West	>360	1.3-1.4	Yes	
10	#12	20-30	North	180-240	1.1-1.2	Yes	
11	#15	10-20	Northeast	180-240	1-1.1	Yes	
12	#16	30-40	Northwest	60-120	1.2-1.3	Yes	
13	#17	20-30	North	120-180	1.1-1.2	Yes	
14	#19	30-40	Southeast	120-180	1.1-1.2	Yes	

particularity of the region, this paper identifies slopes that do not meet the threshold range of the index as potential landslide areas. Table 5 shows the results of element extraction and identification and judgment of 14 possible landslide areas. Finally, based on the environmental factors of land-

slide development, a total of 12 potential landslide areas were identified.

4.5. *Landslide Identification Results.* In order to improve the accuracy of potential landslide identification, this paper will

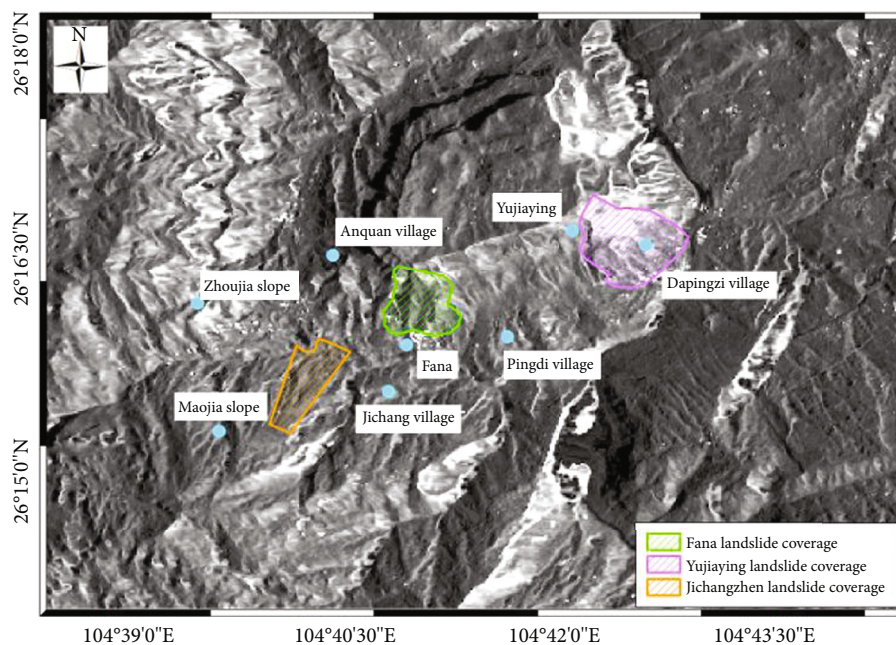


FIGURE 13: The location of the landslide in Jichang Town.

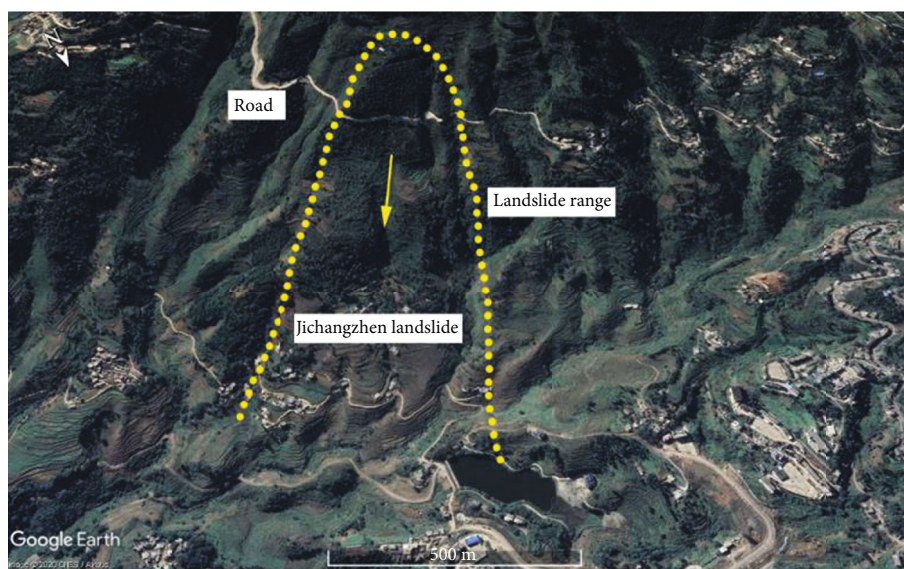


FIGURE 14: The scope of the landslide in Jichang Town.

consider the potential landslide identification results based on time series NDVI and the potential landslide identification results based on landslide development environment elements. If the identified slope body satisfies any one of the following two cases, it is comprehensively determined that the area is not a potential landslide area. First, both of the identification methods determined that it was not a potential landslide. Second, one method cannot be determined, and the other identification method determines that it is not a potential landslide. On the contrary, it is regarded as a potential landslide area. The above rules were used to comprehensively consider and discriminate 14 dangerous deformation areas that may have landslides, and a total of

12 potential landslide areas were identified. In addition, the two deformation areas numbered #1 and #10 in Tongren Research Area were not potential landslide areas.

In summary, this paper combined various methods to investigate the study area, and identified 28 landslide areas (12 potential landslides) and 74 deformation areas (2 unknown settlement areas) caused by other reasons.

5. Landslide Monitoring Results

5.1. Jichang Town Landslide. On July 23, 2019, a huge landslide occurred in Pingdi Village, Jichang Town, Shuicheng County, Liupanshui City. The location of the landslide is

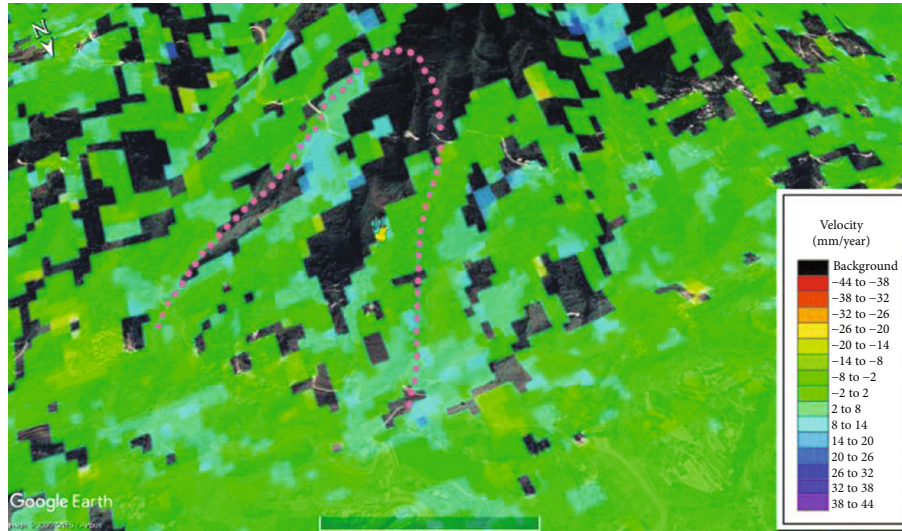


FIGURE 15: Distribution of average displacement rate of landslide in Jichang Town.

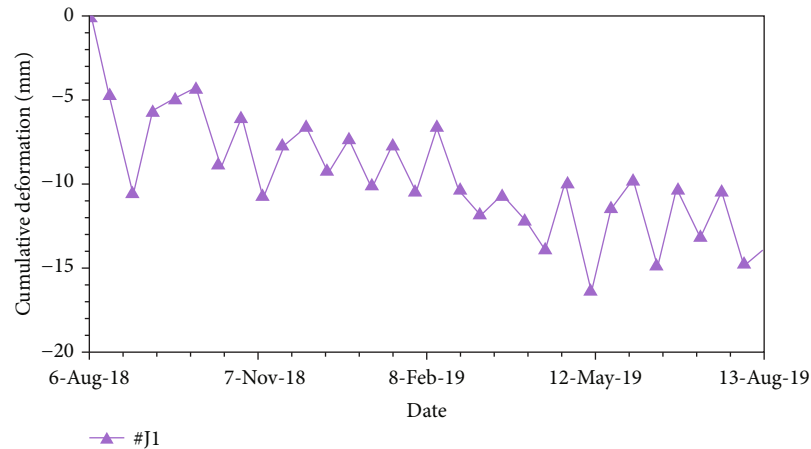


FIGURE 16: Cumulative deformation of landslide sampling points in Jichang Town.

shown in Figure 13, and the range of landslide is shown in Figure 14. In order to find out the possible causes of landslides and prevent the landslide area from continuing to slip, this paper uses SBAS technology to perform inversion calculation on the surface deformation of the landslide area. In this paper, the deformation information of the slope body is extracted, and then InSAR time series analysis is performed to realize the pre-disaster and post-disaster monitoring of the landslide.

Based on the SBAS technology, the displacement rate field of Jichangzhen landslide is obtained, and the obtained displacement rate distribution results are shown in Figure 15. This paper selects sampling point #J1 for the landslide body and extracts the time series deformation results as shown in Figure 16.

It can be seen from Figure 16 that from August 06, 2018 to August 13, 2019, the average displacement rate of the slope is within -14 mm/year and the displacement rate is slow. The cumulative deformation during landslide monitoring is

shown in Figure 15. During the monitoring period, the sampling points of the slope show a slow and continuous downward deformation trend, and the cumulative deformation is within -17 mm. From the time series deformation analysis, it can be seen that there was a weak deformation on the surface before the landslide occurred, but the tiny deformation signal did not attract people's attention.

In the process of landslide identification and investigation of Jichang town and its surrounding areas, two areas with obvious deformation were found not far from the landslide of Jichang town. They are the Yujiaying area and the Fana area. Since the two landslide areas are closer to the landslide in Jichang Town, and the geological structure is also similar, the same disasters as the landslide in Jichang Town will likely occur due to rainfall. Therefore, it is necessary to monitor these two landslide areas.

5.2. Yujiaying Landslide. The Yujiaying landslide and Fana landslide are located on the opposite mountain about 4 km

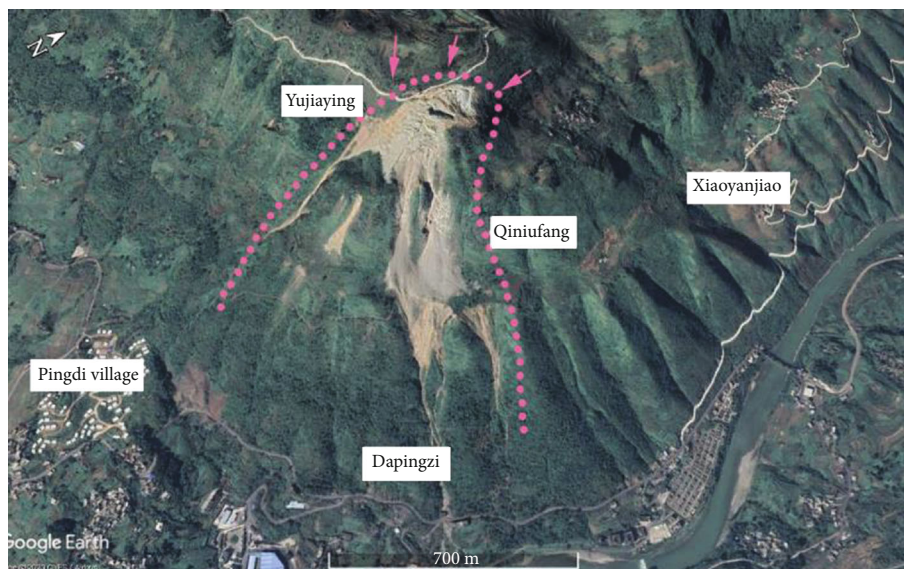


FIGURE 17: Yujiaying Landslide Location.

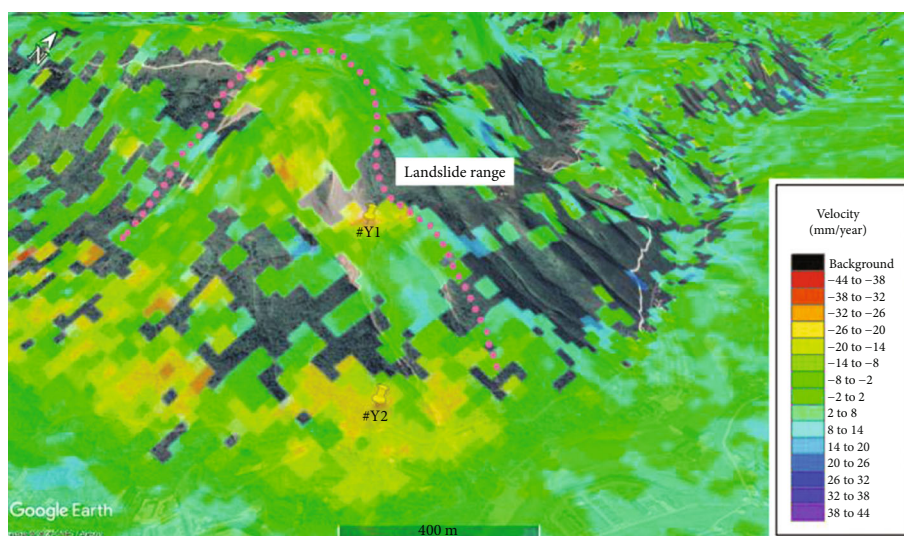


FIGURE 18: Distribution of average displacement rate of Yujiaying landslide.

from the northeast of the landslide body of Jichang Town, that is, the area above Dapingzi Village. The geographical location and landslide range are shown in Figure 17.

1

From the time-series remote sensing images of Yujiaying landslide, it was found that from March 2013 to April 18, 2015, the remote sensing images have clearly identified that the landslide has occurred. The volume of landslides increased in December 2015, and the slope slippage continued until December 2018. In this paper, the SBAS technology is used to obtain the surface deformation information of the Yujiaying landslide area. The surface displacement rate distribution is shown in Figure 18. It can be seen that there are obvious deformation signals in this area, and the displacement rate is within -32 mm/year. The position of the deformation signal corresponds to the landslide body, indicating

that during the monitoring period from August 06, 2018 to August 13, 2019, the slope body is still slipping. If the deformation amount accumulates to a certain degree, it is likely to cause the landslide to happen again. In this paper, the sampling points #Y1 and #Y2 of the slope body are analyzed for the deformation time series. According to Figure 19, it can be seen that the deformation value of the slope body was disturbed before November 2018 and there was a large fluctuation. However, after November 07, 2018, the slope deformation showed a rapid rate of subsidence. As of August 2019, the cumulative amount of subsidence at the sampling point of the slope has reached about -30 mm, and there is still a trend of continued subsidence.

5.3. Fana Landslide. The Fana landslide area is another area that needs to be focused on during the landslide

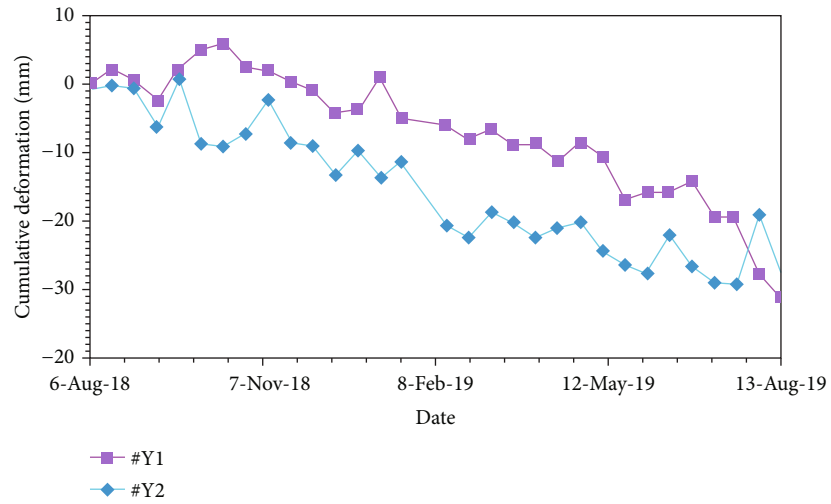


FIGURE 19: Cumulative deformation of landslide sampling points in Yujiaying.

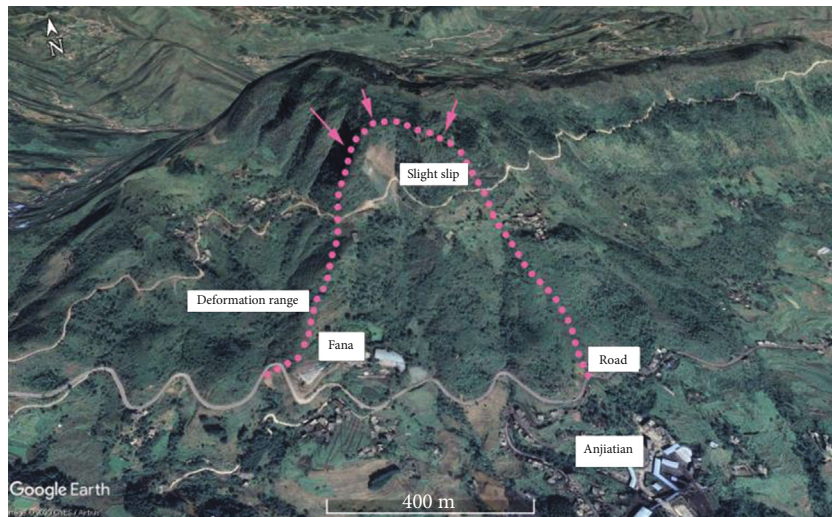


FIGURE 20: The location and historical remote sensing image of Fana landslide.

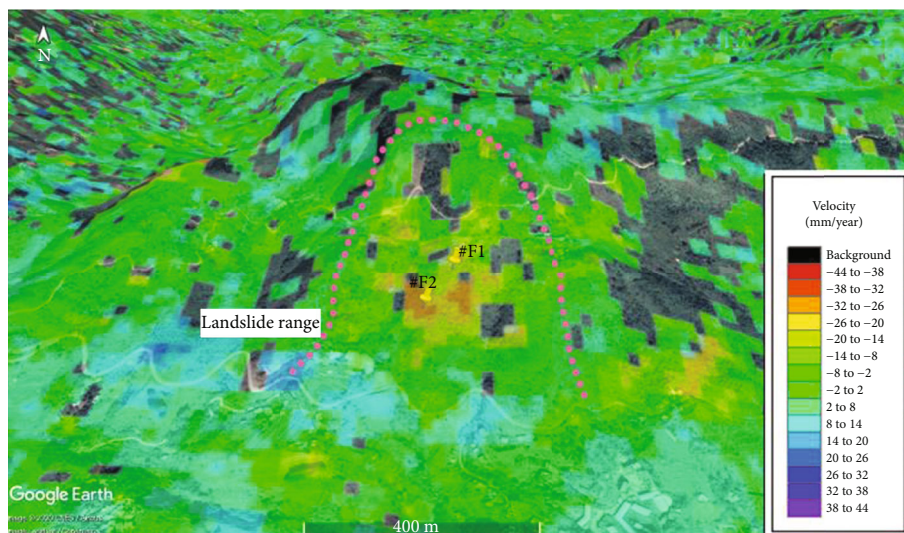


FIGURE 21: Distribution of average displacement rate of Fana landslide.

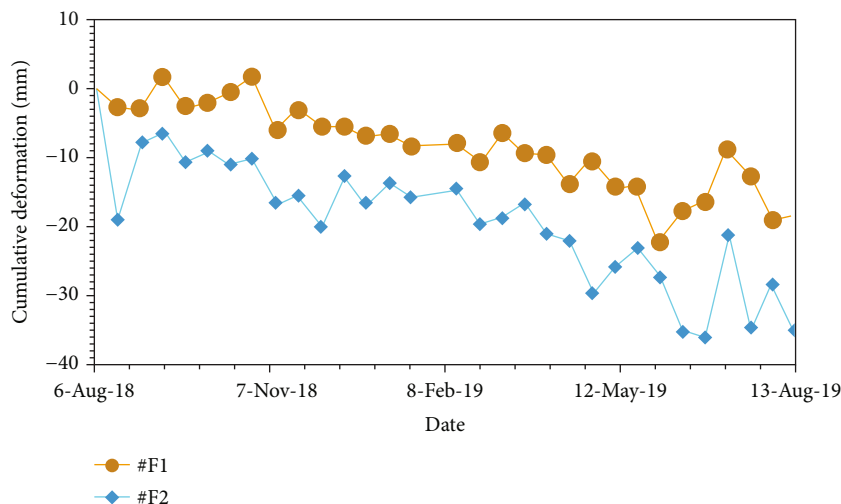


FIGURE 22: Cumulative deformation of landslide sampling points in Fana.

TABLE 6: Statistics of landslide monitoring results.

Research area	Maximum value of surface subsidence	Total number of dangerous areas	Landslide areas	Landslides may exist	Other deformation areas
Liupanshui research area	-64 mm/year	43	11	3	29
Tongren research area	-54 mm/year	40	3	1	36
Guiyang research area	-46 mm/year	19	2	10	7

identification and investigation of the area around the landslide in Jichang Town. Its geographic location is shown in Figure 20. The area is located opposite the landslide in Jichang Town and is very close to the Yujiaying landslide. From the remote sensing historical images of the Fana landslide area, it can be found that before November 14, 2018, there were already signs of landslides in this area, and the slope body of the Fana landslide area is steep, so there is a certain hidden danger of landslide.

In this paper, the displacement rate field of the Fana landslide area is obtained through the SBAS technique. According to the annual average subsidence rate, Figure 21 shows that the displacement rate in this area is above -20 mm/year. The displacement rate of the slope body is faster than that of Jichangzhen landslide, and there are obvious deformation signals at many places on the slope body, so it is necessary to monitor the slope body to further understand the movement of the slope body. In this paper, the sampling point #F1 and sampling point #F2 are selected for the area where a slight slip has occurred, and the time series deformation of the target sampling point is extracted, as shown in Figure 22. The time-series deformation curve of the sampling point shows that only a slow subsidence phenomenon occurs before November 2018, and then there is a significant subsidence phenomenon, and the displacement rate accelerates. The sampling point #F2 reaches the maximum value of subsidence on June 28, 2019 Value -37 mm. In the following two months, the deformation curve has been raised overall. Although it continues to subsidence, the deformation rate tends to slow down. The continuous deformation of the land-

slide will reduce the stability of the slope, and the steep geographical position of the slope will easily cause the landslide to occur. Therefore, it is still necessary to continue to monitor the region in the future.

In summary, the Yujiaying landslide and Fana landslide have already experienced landslides, and there is still a tendency to continue to deform. The geological structure and environment of the two landslide areas are similar to the landslide area of Jichang Town, and they are both located on the slope body with a large vertical drop, so the probability of landslide occurrence is large. And after the landslide in Jichang Town occurs, if traditional methods are used for monitoring, the monitoring instruments may need to be installed on the opposite mountain due to the large monitoring range. Therefore, the stability of the opposite mountain is extremely important. Therefore, the deformation of Yujiaying landslide and Fana landslide should be paid more attention to.

The above is our detailed analysis of landslide monitoring results. Summarize the data we obtained through the experiment, and the main parts are shown in Table 6.

6. Conclusion

This paper takes Guiyang City, Liupanshui City and Tongren City in Guizhou Province as the research areas, and uses SBAS technology to process the radar satellite images of the three areas to determine the dangerous deformation areas. The terrain of Guizhou Province is low from west to East, carbonate rocks are widely distributed, and karst landscape

is widely distributed. Fanjing mountains group in Northeast China is a rift type deposit. There are more than one layer of pillow like basic lava and mantle derived ferrites in the epimetamorphic rock series. According to the analysis of geological environment factors, there is a great possibility of geological disasters in this province. In terms of geographical distribution, geological disasters of different degrees occur in 9 places (prefectures and cities) every year in Guizhou Province, but the most frequent areas are Zunyi, Bijie, Liupanshui, Southwest Guizhou and Tongren. These areas are closely related to geography, geomorphology, geological structure, geotechnical structure and geological climate. Geological disasters in Guizhou Province are mainly small and medium-sized (accounting for more than 90%), and more than major geological disasters occur every year. Since 1993, there have been 58 major geological disasters in the whole province, including 18 cases of death of more than 30 people and loss of more than 10 million yuan. May to September is the high incidence period of geological disasters. Sudden geological disasters mainly occur from May to September, with an average of 40-60 geological disasters per month, accounting for 35-90% of the total number of geological disasters in the whole year. The common types of geological disasters are landslide, collapse, debris flow, land subsidence, ground fissures, etc. the ground fissures in Guizhou are often the reflection of surface collapse, sliding and collapse. Among them, landslides, collapses and debris flows are the most serious geological hazards to people's lives and property. There are not only natural factors causing geological disasters, but also human factors, which are one of the important factors leading to geological disasters. In our study, we found that human factors such as construction or mining also have a great influence.

A total of 102 dangerous deformation areas are identified in this paper. On this basis, this paper uses optical remote sensing images to identify landslides in dangerous deformation zones. Considering the regional particularity, this paper uses typical landslide areas to establish optical image landslide interpretation identification marks and finally identifies 16 landslide areas. At the same time, 72 deformation zones due to construction or mining have been identified, 14 possible landslide areas. Then, landslide identification methods based on NDVI time series analysis and landslide development environment elements are used to identify potential landslides. After comprehensive judgment by these two methods, a total of 12 potential landslide areas were determined. Finally, this article uses SBAS technology to monitor three typical landslides. In this paper, the surface displacement rate field of the landslide area is obtained and the time series deformation analysis is carried out. The study found that the average displacement rate of the two other areas except for the landslide in Jichang Town is relatively large, both above -20 mm/year. Through monitoring and analysis before and after the disaster in Jichang Town, it was found that concentrated heavy rainfall was the main cause of sudden landslides in Jichang Town. During the monitoring period of Yujiaying and Fana landslides, the slopes have obviously declined and there is a tendency to continue to decline. In

view of the incentives of landslides in Jichang Town, these two areas need to be focused on in the future.

The landslide identification method, landslide identification results, and landslide monitoring results used and obtained in this paper provide a reference value for researchers to identify landslides in similar areas, and provide reliable data support and theoretical basis for regional landslide disaster prevention. In future research, obtaining more environmental factors for landslide development, NDVI values obtained by higher resolution remote sensing images, more comprehensive field survey data and measured data will be more conducive to the analysis and research of landslides. At the same time, to ensure the safety of geological environment is conducive to the development of geological disaster prevention.

Data Availability

The data used in our manuscript mainly includes Sentinel-1A satellite data and ALOS World 3D-30 m Digital Elevation Model (AW3D30 DEM) data. The radar imaging satellite is the first dual-constellation satellite developed by ESA and the European Commission for the Copernicus Earth Observation Project. We can access open data sources through the website "<https://scihub.copernicus.eu/>". AW3D30DEM is the global 30 meters DEM data provided by JAXA for free. We can visit from the webpage "<https://www.eorc.jaxa.jp/ALOS/en/aw3d30/data/index.htm>". We hope to be able to share the data of our manuscripts and provide researchers with a way to verify the articles, copy analysis and conduct secondary analyses.

Conflicts of Interest

There is no conflict of interest regarding the publication of this paper.

Acknowledgments

This work is funded by the National Key R&D Program of China (2017YFA0603103), the National Natural Science Foundation of China (41204012, 41974009, 41431070, 41590854, and 41674006), the Science and Technology Plan Project in Fujian Province under grant (2017Y3004), the Key Research Program of Frontier Sciences, Chinese Academy of Sciences (CAS) (Grant nos. QYZDB-SSW-DQC027 and QYZDJ-SSW-DQC042), the State Key Laboratory of Geodesy and Earth's Dynamics Foundation of China under grant (SKLGED2020-2-3-E), Guangdong Province Marine Economic Development (Six Marine Industries) Special Fund Project (GDNRC[2020]050), and Guangdong Provincial Financial Comprehensive Affairs Management Project ([2020]033).

References

- [1] N. van Puymbroeck, R. Michel, R. Binet, J. Avouac, and J. Taboury, "Measuring earthquakes from optical satellite images," *Applied Optics*, vol. 39, no. 20, article 3486, 3494 pages, 2000.

- [2] J. Barlow, Y. Martin, and S. E. Franklin, "Detecting translational landslide scars using segmentation of Landsat ETM+ and DEM data in the northern Cascade Mountains, British Columbia," *Canadian journal of remote sensing*, vol. 29, pp. 510–517, 2003.
- [3] T. R. Martha, N. Kerle, V. Jetten, C. J. van Westen, and K. V. Kumar, "Characterising spectral, spatial and morphometric properties of landslides for semi-automatic detection using object-oriented methods," *Geomorphology*, vol. 116, no. 1-2, pp. 24–36, 2010.
- [4] T. Lahousse, K. T. Chang, and Y. H. Lin, "Landslide mapping with multi-scale object-based image analysis – a case study in the Baichi watershed, Taiwan," *Natural Hazards and Earth System Sciences*, vol. 11, no. 10, pp. 2715–2726, 2011.
- [5] P. Berardino, M. Costantini, G. Franceschetti, A. Iodice, L. Pietranera, and V. Rizzo, "Use of differential SAR interferometry in monitoring and modelling large slope instability at Maratea (Basilicata, Italy)," *Engineering Geology*, vol. 68, no. 1-2, pp. 31–51, 2003.
- [6] P. Farina, D. Colombo, A. Fumagalli, F. Marks, and S. Moretti, "Permanent Scatterers for landslide investigations: outcomes from the ESA-SLAM project," *Engineering Geology*, vol. 88, no. 3-4, pp. 200–217, 2006.
- [7] A. Ferretti, C. Prati, and F. Rocca, "Permanent scatterers in SAR interferometry," *IEEE Transactions on geoscience and remote sensing*, vol. 39, no. 1, pp. 8–20, 2001.
- [8] P. Lu, F. Catani, V. Tofani, and N. Casagli, "Quantitative hazard and risk assessment for slow-moving landslides from Persistent Scatterer Interferometry," *Landslides*, vol. 11, no. 4, pp. 685–696, 2014.
- [9] V. Tofani, F. Raspini, F. Catani, and N. Casagli, "Persistent Scatterer Interferometry (PSI) Technique for Landslide Characterization and Monitoring," *Remote Sensing*, vol. 5, no. 3, pp. 1045–1065, 2013.
- [10] C. Del Ventisette, G. Righini, S. Moretti, and N. Casagli, "Multitemporal landslides inventory map updating using spaceborne SAR analysis," *International Journal of Applied Earth Observation and Geoinformation*, vol. 30, pp. 238–246, 2014.
- [11] W. Frodella, A. Ciampalini, G. Gigli et al., "Synergic use of satellite and ground based remote sensing methods for monitoring the San Leo rock cliff (Northern Italy)," *Geomorphology*, vol. 264, pp. 80–94, 2016.
- [12] E. Intriери, F. Raspini, A. Fumagalli et al., "The Maoxian landslide as seen from space: detecting precursors of failure with Sentinel-1 data," *Landslides*, vol. 15, no. 1, pp. 123–133, 2018.
- [13] F. Liu, T. Chen, J. He, Q. Wen, and Z. Wang, "The research on dryland crop classification based on the fusion of sentinel-1a sar and optical images," *International Archives of the Photogrammetry, Remote Sensing & Spatial Information Sciences*, vol. 42, no. 3, 2018.
- [14] P. Berardino, G. Fornaro, R. Lanari, and E. Sansosti, "A new algorithm for surface deformation monitoring based on small baseline differential SAR interferograms," *IEEE Transactions on geoscience and remote sensing*, vol. 40, no. 11, pp. 2375–2383, 2002.
- [15] B. Hu, H. Li, X. Zhang, and L. Fang, "Oil and gas mining deformation monitoring and assessments of Disaster: Using Interferometric Synthetic Aperture Radar technology," *IEEE Geoscience and Remote Sensing Magazine*, vol. 8, no. 2, pp. 108–134, 2020.